



Wetting behaviour of different tube materials and its influence on scale formation in multiple-effect distillers

Alexander Stärk^a, Katell Loisel^b, Karine Odiot^b, Achim Feßenbecker^b,
Andreas Kempter^b, Stephan Nied^b, Heike Glade^{a,*}

^aTechnical Thermodynamics, University of Bremen, Badgasteiner Str. 1, D-28359 Bremen, Germany, Tel. +49 421 218 64773; Fax: +49 421 218 64771; email: heike.glade@uni-bremen.de (H. Glade)

^bBASF SE, D-67056 Ludwigshafen, Germany

Received 14 April 2014; Accepted 16 June 2014

ABSTRACT

Multiple-effect distillation (MED) plants with horizontal tube falling film evaporators for sea water desalination exhibit relatively high heat transfer coefficients achieved by film flow under clean surface conditions. However, they are susceptible to heat transfer deterioration and scale formation accompanied by film breakdown. Thus, maintaining all heated tubes in a fully wetted state is one of the key issues to be considered in designing falling film evaporators. Surface tension, hydrophilicity, hydrophobicity and wettability of materials play an important role in scale formation. The wetting rate, that is the brine mass flow rate on one tube per unit tube length, is one of the most important parameters in the design and operation of MED plants. It has an impact on heat transfer, tube bundle design, scale formation, the capital and operational costs of the plant and its operational flexibility. Thus, it is very important to acquire a better understanding of the wetting behaviour and the impact of different tube materials, various process parameters and sea water properties on tube wetting. The wetting behaviour of different tube materials such as aluminium brass, copper–nickel 90/10 and aluminium alloy AlMg2.5, which are commonly used in MED plants, was investigated in a horizontal tube falling film evaporator in pilot plant scale. In tests with stepwise increasing and decreasing wetting rate, pictures of the film flow over the horizontal tubes were taken and the percentages of the wet surface area were evaluated by means of an image processing software. The tube surfaces were characterized by measuring contact angles and determining surface free energies. Furthermore, the horizontal tube falling evaporator was used to study the effect of the wetting rate on composition and quantity of mixed salt scale. Experiments were performed with artificial sea water at wetting rates from 0.14 kg/(s m) down to 0.025 kg/(s m) for different tube materials such as aluminium brass, copper–nickel 90/10 and AlMg2.5. New insights into the wetting behaviour of different tube materials and the influence of the wetting rate on scale formation in the horizontal tube falling film evaporators are given. The effects of various process parameters such as wetting rate, temperature and salinity on the wettability of typical tube materials and the effect of

*Corresponding author.

*Presented at the Conference on Desalination for the Environment: Clean Water and Energy
11–15 May 2014, Limassol, Cyprus*

the wetting rate on composition and quantity of mixed salt scale are presented and discussed.

Keywords: Tube wetting; Wetting rate; Scale formation; Calcium carbonate; Magnesium hydroxide; Multiple-effect distiller

1. Introduction

In multiple-effect distillation (MED) plants with horizontal tube falling film evaporators for sea water desalination, a major problem encountered is the scale formation on the outside of the tubes, which prevents the use of mechanical cleaning methods such as ball cleaning systems. The crystalline scale formed on the heat transfer surfaces reduces the overall heat transfer coefficient. Thus, the efficiency of the distiller decreases and the distillate production drops at a certain limit. Assuming a scale layer of calcium carbonate with a thermal conductivity between 1.5 and 2.9 W/(m K) [1], a layer thickness of only 150–290 μm would result in a fouling resistance of 0.1 ($\text{m}^2 \text{K}$)/kW which is often assumed in the design of multiple-effect distillers [2]. Achieving effective scale control is consequently a major concern of the desalination industry.

Sea water is a multi-component electrolyte solution. Scale formation is caused by co-precipitation of different calcium- and magnesium-containing salts such as calcium carbonate, magnesium hydroxide and calcium sulphate. The solubilities of these salts decrease with the increasing temperature. There are many factors influencing crystallization fouling which can be classified into the three following major categories [3,4]:

- Operating parameters (surface and bulk temperature, pressure, heat flux and fluid dynamics such as flow velocity and flow regime);
- solution composition (components, concentrations, pH, supersaturation and suspended particles); and
- heat exchanger characteristics (surface free energy, topography and surface roughness).

Common materials used for heat exchanger tubing in MED plants are copper–nickel 90/10, aluminium brass, titanium grade 2, aluminium alloy AlMg2.5 (alloy EN AW 5052) and highly corrosion-resistant stainless steel grades such as SS 1.4565. The choice of tube material affects the wettability, the adhesion forces between surface and deposit as well as the induction time of crystallization fouling.

Wettability studies usually involve the measurement of contact angles which indicates the degree of

wetting when a solid and liquid interact [5]. Calculations based on measured contact angles yield the solid surface free energy, which quantifies the wetting characteristics of a solid material.

The contact angle is the angle formed by the solid–liquid interface and the liquid–vapour interface measured from the side of the liquid. The contact angle is the resultant of adhesive and cohesive forces and provides an inverse measure of the wettability of the surface. A contact angle less than 90° indicates that the wetting of the surface is favourable, and the liquid will spread over a large area on the surface; while a contact angle greater than 90° generally indicates that the wetting of the surface is unfavourable so the liquid will minimize its contact with the surface and form a compact liquid droplet [5].

As described by Young [6], the contact angle of a liquid drop on an ideal solid surface is defined by the mechanical equilibrium of the drop under the action of three interfacial tensions:

$$\gamma_{lv} \cos \theta_Y = \gamma_{sv} - \gamma_{sl} \quad (1)$$

where γ_{lv} , γ_{sv} and γ_{sl} are the liquid–vapour, solid–vapour and solid–liquid interfacial tensions, respectively, and θ_Y is referred to as Young's contact angle.

The phenomenon of wetting is more than just a static state. The liquid moves to expose its fresh surface and to wet the fresh surface of the solid in turn [5]. The dynamic contact angle between a solid and a liquid is the contact angle which occurs in the course of the wetting and de-wetting process. In particular, the contact angles formed by expanding and contracting the liquid are referred to as the advancing contact angle and the receding contact angle, respectively. The advancing contact angle is always larger than or equal to the receding contact angle. The difference between the advancing angle and the receding angle is called contact angle hysteresis. It is generally believed that the contact angle hysteresis arises from surface roughness and/or heterogeneity [5]. A pure liquid in the saturated vapour phase on an ideal, chemically and topographically homogeneous solid forms an ideal contact angle as described by Young's equation. With real solids, liquids and ambient conditions, the contact angle can vary as a function of time and location. If

the effect of the contact time and location is to be minimized, then the advancing angle is usually measured. Technical wetting processes are often dynamic processes which are better modelled by means of dynamic contact angle measurements. On smooth but chemically heterogeneous solid surfaces, the experimental advancing contact angle might be expected to be a good approximation of Young's contact angle [5]. There are no general guidelines regarding how smooth a solid surface must be for surface roughness not to have an obvious impact on the contact angle [5].

One of the most important parameters in the design of multiple-effect distillers is the wetting rate, Γ . It can be defined as the falling film mass flow rate on one side or on both sides of a horizontal tube per unit tube length. In the following, the wetting rate is expressed as the mass flow rate, \dot{m} , on both sides of a horizontal tube per unit tube length, L :

$$\Gamma = \frac{\dot{m}}{L}. \quad (2)$$

Different definitions of the film Reynolds number can be found in the literature. In the following, the film Reynolds number Re_F given by:

$$Re_F = \frac{\Gamma}{\eta} \quad (3)$$

is used with η as the dynamic viscosity of the liquid. The film Reynolds number can also be expressed as:

$$Re_F = \frac{\dot{m}}{L \eta} = \frac{2 \bar{u} \delta \rho}{\eta} \quad (4)$$

where \bar{u} is the average flow velocity in the film, δ is the film thickness and ρ is the density of the liquid.

The wetting rate has an impact on heat transfer, tube bundle design (width and height of the tube bundle), scale formation, the capital and operational costs of the plant and its operational flexibility. The wetting rate determines whether the tube surface is completely covered with water or the thin sea water film breaks down and dry patches occur. Moreover, the wetting rate strongly influences the film thickness and the flow regime on the tubes (laminar, wavy-laminar, turbulent flow), the pattern of liquid flow between adjacent horizontal tubes (droplet dripping, liquid jets, liquid sheets), and thus heat transfer. The brine mass flow rate is increasingly reduced towards the lower tubes due to the evaporation when the brine falls down to

successive heated tubes. The liquid film on a tube breaks down when the flow rate falls below a certain minimum.

The sea water film on the horizontal tubes creates a resistance to heat transfer and it should be as thin as possible, that is the wetting rate should be as low as possible. MED plant manufacturers (e.g. [7]) and operators strive for low wetting rates because low wetting rates are beneficial for the heat transfer, the thermal and the electrical energy consumption (pumping power). On the other hand, dry patches, that is areas that transmit essentially no heat and thus reduce thermal performance, should never appear. Scale formation preferably starts at the edges of the dry patches because they induce full local evaporation of the sea water and a salt concentration beyond the scale formation thresholds [7]. Baujat and Bukato [7] raise the question to what extent the height of the tube bundle can be increased without risk if the quality of sea water distribution is not consistent from top to bottom and what will be the long term operation of the MED plant if scaling cannot be controlled. Furthermore, MED plants with high thermal efficiencies require large heat transfer surface areas which must be wetted. Thus, it is difficult to design an MED plant with high thermal efficiency with respect to tube wetting and scale formation [8]. Furthermore, the design of MED plants with small capacities is also particularly difficult because it is hard to find reasonable tube bundle dimensions (height and width of the tube bundle) if relatively high wetting rates are required [9].

The mass flow rate per unit tube length, that is the wetting rate, affects the thickness of the thin film and the flow velocity of the film (Eq. (4)), which in turn influences the scaling process. Growth of a crystal scale layer involves mass transport of the crystallizing constituents towards the solution–crystal interface followed by a crystallization surface reaction [10]. The mass transport step is attributed to the molecular diffusion of ions through the laminar boundary layer at the surface. The attachment step is described by the strongly temperature-dependent surface integration of ions into the crystal lattice which has often been found to follow Arrhenius type rate equation [11]. Fluid flow velocity can either promote or suppress the severity of the scaling process. On the one hand, an increase in the velocity enhances the mass transfer rate in turbulent flow and thus acts to augment the scaling rate. On the other hand, an increase in the velocity also intensifies the interfacial shear stress on the scale surface, counteracting the adhesion forces that act to incorporate freshly formed material into the scale structure [10].

Crystallization fouling of calcium carbonate has been mainly studied in turbulent, forced convection systems. It can be controlled by mass transfer, by chemical reaction at the heat transfer surface or by both mechanisms [12]. Hasson et al. [13] reported that CaCO_3 crystallization fouling in an annular test section under turbulent, constant heat flux conditions is controlled by the rate of diffusion as fouling rate increased with the increasing Reynolds number. Instead, Augustin and Bohnet [14] considered crystallization fouling of CaCO_3 in an annular duct to be controlled by surface integration. Helalizadeh et al. [12] proposed that the fouling process is diffusion controlled at low flow velocities of the mixed CaCO_3 – CaSO_4 solution and surface integration controlled at high flow velocities. Fouling behaviour of the same salt may therefore vary in different systems and operation conditions which make it essential to understand the fouling behaviour in the system of interest in order to reduce fouling [11].

In industrial practice, it is known that dry patches should be avoided and that the wetting rate has an influence on scale formation in horizontal tube falling film evaporators, but the effects of the wetting rate on scale formation have not systematically been investigated in detail. The objective of this study is to contribute to a better understanding of the wetting behaviour of different tube materials and the effects of the wetting rate on scale formation. A better insight may help to design and operate more efficient heat exchangers.

In the following, the experimental set-up is described and the results of the experimental study are shown and discussed.

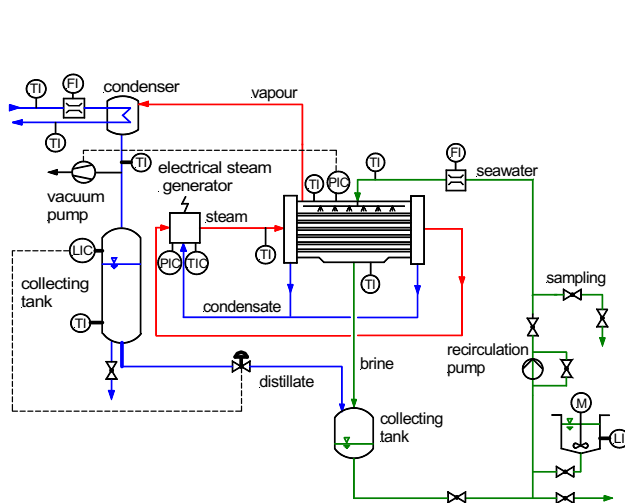


Fig. 1. Schematic diagram of the test rig.

2. Materials and methods

2.1. Test rig

The experimental studies were performed in a horizontal tube falling film evaporator in pilot plant scale. Fig. 1 shows a schematic diagram of the test rig.

As shown in Fig. 2, the main part of the test rig is an evaporator fitted with a bank of 6 horizontal tubes arranged below each other with a tube pitch of $s = 50$ mm. Saturated steam from an electrical steam generator is introduced into the tubes and condensed under vacuum conditions while the heat is transferred to the evaporation side. The test liquid is evenly distributed onto the first tube by means of a toothed overflow weir and trickles down by gravity forming a thin film flow over the horizontal tubes. The mass flow rate per unit tube length can be varied in a wide range. The enthalpy of condensation allows the test liquid to be preheated to the boiling point on the upper tube and then part of it to be evaporated on the lower tubes. The generated vapour is condensed in a plate heat exchanger. After leaving the evaporator, the test liquid flows into a collecting tank and is mixed with the distillate. Then, the test liquid is recirculated by a pump.

CO_2 released from evaporating sea water and ambient air potentially penetrated into the evaporator are extracted by means of a vacuum pump which maintains the saturation pressure in the evaporator shell. The pilot plant provides conditions for CO_2 release from sea water very similar to those in industrial multiple-effect distillers. CO_2 release shifts the pH value of the sea water to higher values and influences the carbonate system.

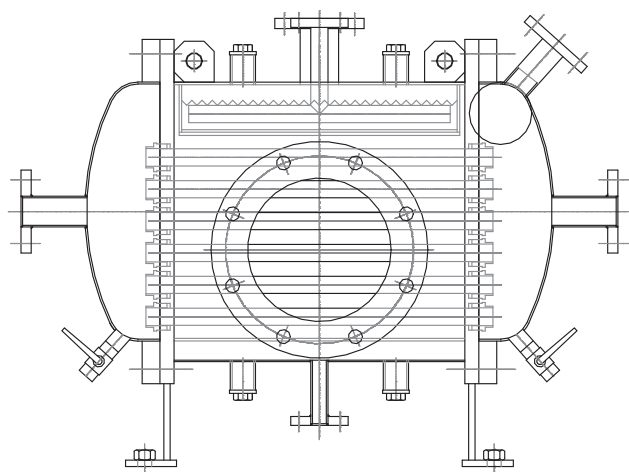


Fig. 2. Drawing of the horizontal tube falling film evaporator.

The test rig is equipped with various temperature, pressure and flow rate measuring devices in order to monitor and control the process. Control of the apparatus is completely automatic so that it requires a minimum of supervision. This is an important feature because continuous, steady operation over long periods is essential to obtain reproducible scaling results.

The tubes can be removed from the tube sheets in order to renew the tubes, to test different tube materials and to analyse the adherent scale. On both sides of the evaporator, inspection glasses are installed which allow for a visual observation of the wetting behaviour.

2.2. Test liquids

For investigating scale formation, test series were performed with artificial sea water. The wetting behaviour of different tube materials was studied using artificial sea water as well as deionized water.

The preparation of artificial sea water was based on salt mole fractions for standard artificial sea water as suggested in the formulation by Kester et al. [15]. After mixing the salts and stirring the solution, the artificial sea water was aerated. The aeration tended to equilibrate the solution with atmospheric gases and removed the excess CO_2 resulting from the conversion of HCO_3^- to CO_3^{2-} . The pH of the artificial sea water after aeration was between 8.1 and 8.3.

The salinity of ocean surface waters throughout the world is fairly uniform about 35 g/kg. In areas with a high level of rainfall or river runoff, the salinity is less. In areas with higher rates of evaporation, the salinity is higher, for example in the Persian Gulf. In sea water, the relative proportion of the major ions compared to the salinity remains constant [16]. The composition of artificial sea water is within 1 mg/kg of natural sea water for all the major constituents [15]. Therefore, the composition of the artificial sea water used in the experiments is representative for natural sea water with respect to the salts.

Experiments were performed with artificial sea water having a salinity of 65 g/kg simulating the concentrated sea water on the bottom tubes in industrial MED plants taking into account a typical concentration factor between 1.3 and 1.6. Sea water with a salinity of 65 g/kg has an ionic strength of 1.39 mol/kg. For comparison, average sea water having a salinity of 35 g/kg has an ionic strength of 0.72 mol/kg.

2.3. Tube materials

In the horizontal tube falling film evaporator, seamless tubes made of copper–nickel 90/10, alumin-

ium brass and the aluminium alloy AlMg2.5 containing 2.4–2.8% magnesium, which are typical tubing materials in MED plants, were used. Additionally, tubes made of the stainless steel grade 1.4301 were used.

The outer diameter of the tubes was $d_0 = 25$ mm and $d_0 = 26.9$ mm for SS 1.4301, respectively. The effective length was $L = 453$ mm. For studying the wetting behaviour and scale formation, the tubes were used with their typical surface topography as delivered by the tube suppliers. Only the SS 1.4301 tubes used for the tests on the effects of the wetting rate on scale formation were sandblasted. The surface roughness was determined using a tactile stylus unit (perthometer). The tube materials, thermal conductivities, outer diameters, wall thicknesses and surface roughnesses are summarized in Table 1.

2.4. Tube surface characterization

The tube surfaces were characterized by measuring contact angles and determining surface free energies. Before measuring the contact angle, the surface was thoroughly cleaned with isopropyl alcohol to remove any deposits, grease, oil, etc. The advancing contact angle was measured using a drop shape analysis (DSA) instrument (Krüss, contact angle measurement system G2). A sessile drop is formed on the surface by means of a syringe needle, and the volume of the drop is slowly increased. In doing so, the interface migrates outwards. By means of a CCD camera and a data processing system, the image of the liquid droplet is digitized. A contour recognition is initially carried out, and afterwards, the drop shape is fitted to the contour.

The surface free energy was determined on the basis of the contact angle measurements with three test liquids and Young's equation (Eq. (1)). The solid–liquid interfacial free energy between tube surface and droplet in Young's equation was calculated using the geometric mean approach (Owens–Wendt–Rabel–Kaelble method). For metallic surfaces, the geometric and harmonic mean approaches to calculate the solid–liquid interfacial free energy should be favoured because they are state of the art and have been used frequently in many research areas for the combination of wetting and adhesion [17].

2.5. Chemical and structural characterization of the scale layers

The crystalline scale layers formed on the outside of the tubes of the evaporator were characterized at

Table 1
Tube data

Alloy	UNS no.	Thermal conductivity (W/(m K))	Outer diameter (mm)	Wall thickness (mm)	Surface roughness R_a (μm)
CuNi 90/10	C70600	52 (@ 20°C) 60 (@ 100°C)	25	1.0	0.28
Al brass	C68700	112 (@ 100°C)	25	1.0	0.44
AlMg2.5	A95052	146 (@100°C)	25	1.25	0.46
SS 1.4301	S30400	15 (@ 20°C) 16 (@ 100°C)	26.9	2.0	0.16 (wetting experiments) 3.17 (scaling experiments)

the laboratories of BASF by various methods to obtain chemical, structural and quantitative information. The scale formed on the fifth tube from the top of the tube bank was analyzed using scanning electron microscopy (SEM) in combination with energy dispersive X-ray spectroscopy (EDXS) and wide-angle X-ray diffraction (XRD) to provide qualitative information on structural and chemical characteristics/properties of the scale, especially about composition, crystal structure, crystal size and orientation and crystal perfection.

The amounts of calcium and magnesium in the scale were detected by atomic absorption spectroscopy (AAS). To this end, the scale of the fourth tube was dissolved in a hot solution of acetic acid and the concentrations of Ca^{2+} and Mg^{2+} ions in the solution were measured using AAS.

Additionally, the scale thickness was determined on the outside of the third tube. It was measured 10 times each at 4 different positions around the tube and at 9 different positions along the tube with a gauge (MiniTest 2100, ElektroPhysik, Germany) designed for non-destructive and precise coating thickness measurement.

2.6. Test procedure

The wetting behaviour of different tube materials (wetting experiments) and the effects of the wetting rate on scale formation (scaling experiments) were studied. Prior to each test, the tube surface was thoroughly cleaned with soap solution, rinsed with plenty of deionized water, and cleaned again with isopropyl alcohol to remove any deposits, grease, oil, etc.

2.6.1. Wetting experiments

Starting with completely dry tube surfaces, the wetting rate was stepwise increased with increments

of about 0.005–0.01 kg/(s m). At each wetting rate, pictures were taken of the film flow over the top 5 tubes at certain time intervals. When a fully wetted state was reached, the wetting rate was stepwise decreased with decrements of about 0.005–0.01 kg/(s m) and pictures were taken of the film flow at certain intervals of time.

The percentages of the wet surface areas on the tube surfaces were evaluated by means of image processing software. The film flow over about 63% of the tube length was considered in the picture analysis. The non-relevant areas between adjacent tubes were cut off with a graphics editing software (Adobe Photoshop, Adobe Systems, USA). Afterwards, the dry patches were marked with an image processing software (ImageJ, National Institutes of Health, USA), and the percentages of the wet surface area were calculated.

The inspection glasses of the falling film evaporator are partially steamed up and covered with water droplets during operation. Thus, a clear analysis of the pictures taken through the inspection glasses is difficult. Therefore, the wetting tests were performed without inspection glasses at ambient pressure. The temperature of the test solution was varied. The wetting behaviour of different tube materials with deionized water and sea water was analyzed and compared.

2.6.2. Scaling experiments

All scale formation experiments were performed with 240 L of artificial sea water with a salinity of 65 g/kg for a test period of 50 h. In previous experiments, different volumes of test solution and time periods were tested. Experiments with 240 L of test solution and a test period of 50 h were found to be favourable because the period is long enough to find differences in scale formation and supersaturation levels are still high enough.

In order to consider a possible extension of the operating range of multiple-effect distillers towards higher top brine temperatures, experiments were performed at an evaporation temperature of $t_{EV} = 75^\circ\text{C}$ exceeding the top brine temperatures currently used in industrial MED distillers. The difference between the condensation temperature t_{CO} inside the tubes and the evaporation temperature t_{EV} outside was $t_{CO} - t_{EV} = 5^\circ\text{C}$.

3. Results and discussion

In the following, the wetting behaviour of different tube materials is presented. Furthermore, the effects of the wetting rate on the composition and quantity of scale formed on the tube surfaces are shown and discussed.

3.1. Contact angles and surface free energies

Fig. 3 shows the advancing contact angles of water on the tube materials based on the DSA. The contact angles of water on the metals decrease in the order of $\text{CuNi 90/10} > \text{SS 1.4301} > \text{AlMg2.5} > \text{Al brass}$. Decreasing contact angles indicate an improved wettability of the surfaces.

The surface free energies of the metals determined with Young's equation on the basis of the contact angle measurements are shown in Fig. 4. The solid-liquid interfacial free energy between tube surface and droplet in Young's equation was calculated using the geometric mean approach (Owens–Wendt–Rabel–Kaelble method). The increasing polar part of the surface free energy indicates that the degree of wetting of the surface with water might increase in the order of $\text{CuNi 90/10} < \text{SS 1.4301} < \text{AlMg2.5} < \text{Al brass}$.

3.2. Wetting hysteresis and influence of wetting time and tube position on wetting behaviour

The wetting experiments were performed in the horizontal tube falling film evaporator as described in

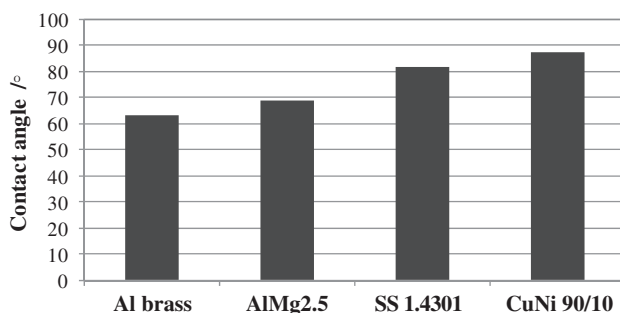


Fig. 3. Advancing contact angles with water.

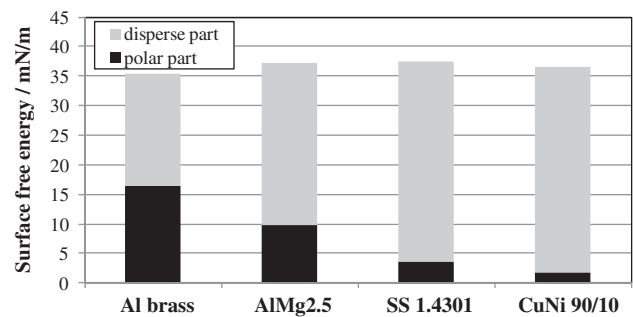


Fig. 4. Surface free energies of the tube materials.

Section 2.6.1. Fig. 5 shows the percentages of the wet surface areas depending on the wetting rate for CuNi 90/10 tubes with deionized (DI) water at a temperature of 27°C . At each wetting rate, pictures of the tubes were taken immediately (0 min), after 10 min and after 20 min. Except for the results in Fig. 6, the top tube was not taken into account in the picture analysis because it was observed that the top tube serves as some sort of distribution tube for the liquid flow.

The wet surface area increases with wetting time at a constant wetting rate, as shown in Fig. 5. The technical wetting process of falling films on horizontal tubes is a dynamic process, and wetting time has an influence. In the following, results are shown for a relaxation time of 10 min because the differences in the percentages of the wet surface areas between 10 and 20 min are very small.

Fig. 5 also shows the hysteresis between the wet surface areas occurring at the increasing and decreasing wetting rate. Starting with dry tube surfaces, the wet surface area increases with the increasing wetting rate until the tube surface is completely covered by a

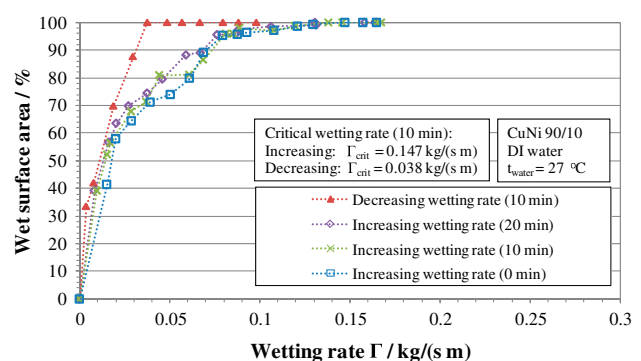


Fig. 5. Wetting behaviour of CuNi 90/10 tubes depending on wetting time and increasing and decreasing wetting rates.

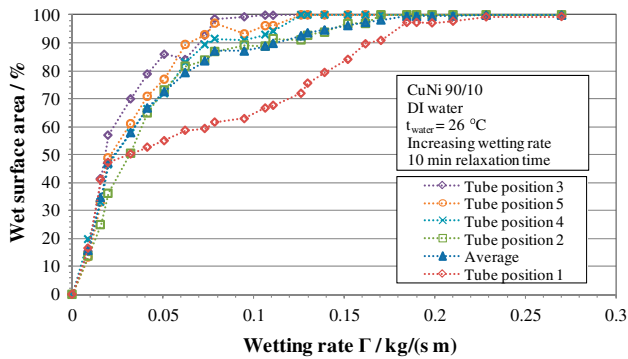


Fig. 6. Wetting behaviour of CuNi 90/10 tubes depending on the tube position.

thin water film at a critical wetting rate of $\Gamma_{crit} = 0.147 \text{ kg/(s m)}$. However, starting from a fully wetted state and decreasing the wetting rate, the whole tube surface stays wet until the film breaks down at $\Gamma_{crit} = 0.038 \text{ kg/(s m)}$. The effect of wetting time and the wetting hysteresis were observed for each tube material. Rio and Limat [18] investigated dry patches in a film flowing over an inclined plate and also observed a wetting hysteresis which was explained by the contact angle hysteresis.

The liquid flow distribution was improved by fixing thin wires at the toothed overflow weir to ensure that the jets of the test liquid run down the wires in even distances. Fig. 6 shows the wetting behaviour of the top five CuNi 90/10 tubes. It is evident that the wetting of the top tube differs from the other tubes. Gebel [19] and Fujita and Tsutsui [20] also observed that the top tubes in horizontal tube falling film evaporators serve as liquid distribution tubes.

3.3. Impact of tube material and test liquid on wetting

Wetting experiments were performed with deionized water and sea water on different tube materials. Sea water with a salinity of 65 g/kg has a slightly higher surface tension than water at the same temperature. Furthermore, the dynamic viscosity of sea water is higher than the one of water at the same temperature. Consequently, the film Reynolds number of sea water given by Eq. (3) is lower at the same wetting rate. Fig. 7 shows the percentages of the wet surface areas depending on the film Reynolds number.

The wettability of the different alloys with deionized water in the pilot plant was found to be in the order of $\text{Al brass} > \text{AlMg2.5} > \text{CuNi 90/10} > \text{SS 1.4301}$. For sea water, the wettability of the different alloys was in the order of $\text{AlMg2.5} > \text{Al brass} > \text{CuNi 90/10} > \text{SS 1.4301}$.

The measured contact angles, shown in Fig. 3, also indicate that the wetting of the Al brass and AlMg2.5 tube surfaces is more favourable than the wetting of the SS 1.4301 and CuNi 90/10 surfaces. The measured contact angles of SS 1.4301 and CuNi 90/10 are similar, and surface roughness and/or physical/chemical reactions between the solid and the liquid may cause a better wetting of the CuNi 90/10 tube surface than that of the SS 1.4301 tube surface.

At the same film Reynolds number, all the tube materials show higher percentages of the wet surface area with artificial sea water than with deionized water, as shown in Fig. 7. The higher values of surface tension and viscosity of sea water would rather lead to a decrease in the percentages of the wet surface area compared to deionized water. A higher surface tension of the liquid means that the liquid would minimize the contact with the solid surface and the wet surface area would get smaller. However, the results suggest that physical/chemical effects between solid surface and sea water cause an increase in the wet surface areas.

3.4. Impact of temperature on wetting

The wetting experiments were performed with deionized water at ambient pressure and a fluid temperature of 29°C as well as with deionized water on heated tubes (condensing steam inside tubes) at ambient pressure and a fluid temperature of 63°C . The dynamic viscosity of water decreases with the increasing temperature. Consequently, the film Reynolds number of hot water given by Eq. (3) is higher than the one of cold water at the same wetting rate. Fig. 8 shows the effect of the film Reynolds number on the percentages of the wet surface area for cold and hot deionized water.

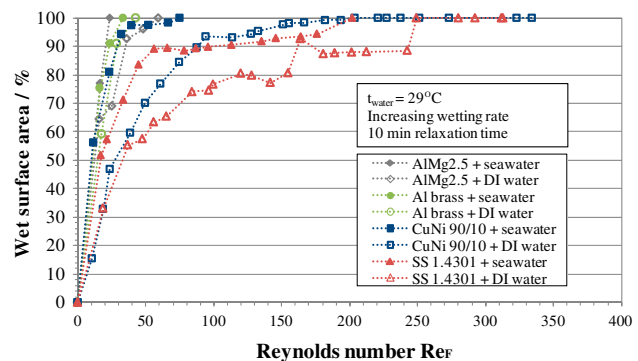


Fig. 7. Effects of the tube material and the test liquid on the wetting behaviour.

For CuNi 90/10 and AlMg2.5 tubes, the degree of wetting with hot water is higher than with cold water. The surface tension of water decreases with the increasing temperature, which reduces the contact angle and tends to increase the degree of wetting. If wettability with cold water is already high as in the case of Al brass, it will be difficult to show an improved wettability with hot water at low wetting rates in such a dynamic process.

3.5. Effect of wetting rate on scale formation

In order to study the effect of the wetting rate on scale formation, experiments were performed with artificial sea water at an evaporation temperature of $t_{EV} = 75^\circ\text{C}$ and a condensation temperature of $t_{CO} = 80^\circ\text{C}$. Tubes made of CuNi 90/10, Al brass, AlMg2.5 and SS 1.4301 were used. The tube surface of the stainless steel tubes was sandblasted. The wetting rate was varied in a range between 0.025 and 0.14 kg/(sm), which corresponds to the film Reynolds numbers of 56–313. Some researchers assume (e.g. [21]) that the Reynolds numbers indicating the transition point from laminar to wavy-laminar and to turbulent flow, originally developed for falling films on vertical surfaces, also apply to falling films on horizontal tubes. Applying correlations for the transition between laminar flow and wavy-laminar flow given by Kapitza [22] and for the transition between wavy-laminar and turbulent flow given by Wilke [23], the film flow is in the wavy-laminar regime. The tube surfaces were completely covered with a thin film during the experiments. Dry patches did not occur according to the visual observation.

All tubes exhibited a relatively uniform scale layer after the experiments. SEM and EDXS analyses reveal that the tube surfaces were covered with a two-layer

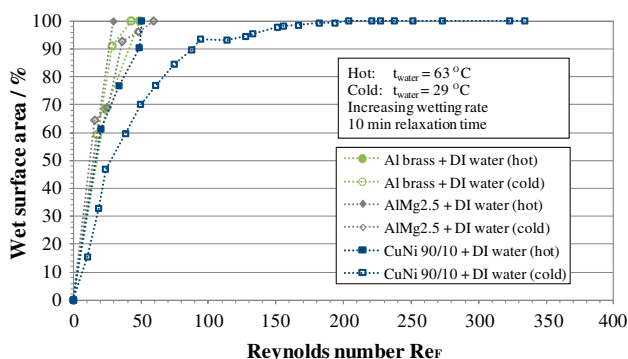


Fig. 8. Effect of temperature on wetting of different tube materials.

scale comprising a thin, flaky magnesium-rich base layer underneath a thick layer of calcium carbonate crystals in the form of aragonite. In previous experiments [24], XRD analyses mainly indicated $\text{Mg}(\text{OH})_2$ (brucite) or iowaite (layered double hydroxide, also known as hydrotalcite-like compound) in the magnesium-rich scale. Iowaite, having a structure based on the brucite structure, may be formed in the presence of corrosion products.

Fig. 9 shows the effect of the wetting rate on the mass of calcium per unit tube surface area, which was determined by AAS. The mass of calcium per unit tube surface area increases with the decreasing wetting rate for all the tube materials. After a test period of 50 h, most CaCO_3 scale was found on the CuNi 90/10 and SS 1.4301 tubes. Less calcium-containing scale formed on the AlMg2.5 tubes.

The effect of the wetting rate on the mass of magnesium in the scale per unit tube surface area, which was determined by AAS, is shown in Fig. 10. While the magnesium mass per unit tube surface area was low on the CuNi 90/10, Al brass and SS 1.4301 tubes and the quantity of the magnesium-containing scale did not notably change at different wetting rates, the magnesium mass in the scale was relatively high on the AlMg2.5 tubes. In previous experiments [25], the magnesium content found on aluminium alloy AlMgSi0.5 (alloy EN AW 6060) tubes was also higher than on CuNi 90/10, Al brass and SS 1.4565 tubes. The results suggest that the magnesium-containing scale has a higher affinity to aluminium alloys than to copper alloys or stainless steel grades.

Fig. 11 shows the effect of the wetting rate on the average thickness of the scale layer. Since the scale

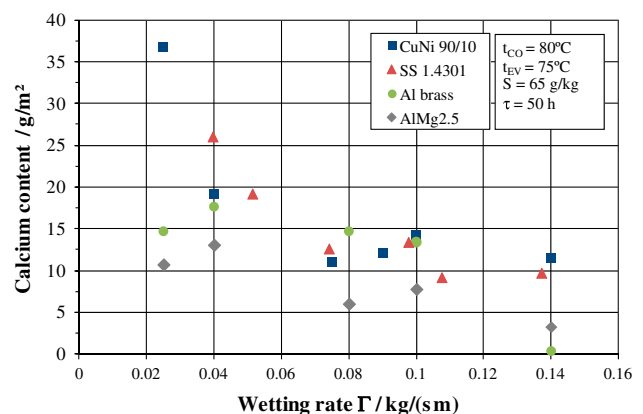


Fig. 9. Effects of the wetting rate on the masses of calcium in the scale per unit tube surface area for different tube materials after a test period of 50 h, $t_{EV} = 75^\circ\text{C}$, $t_{CO} = 80^\circ\text{C}$, $S = 65 \text{ g/kg}$.

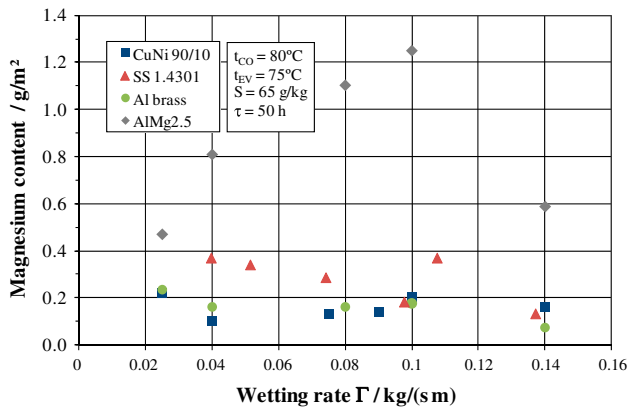


Fig. 10. Effects of the wetting rate on the masses of magnesium in the scale per unit tube surface area for different tube materials after a test period of 50 h, $t_{EV} = 75^\circ\text{C}$, $t_{CO} = 80^\circ\text{C}$, $S = 65 \text{ g/kg}$.

layer mainly consists of calcium carbonate in the form of aragonite and to a lesser extent of magnesium-containing compounds, the average scale thickness increases with the decreasing wetting rate which corresponds to the increasing calcium content on the tube surface, as shown in Fig. 9.

Crystallization fouling is a complex process, and flow velocity has opposing effects. In turbulent flow, an increase in the flow velocity enhances mass transfer. On the other hand, an increase in the velocity also intensifies the interfacial shear stress on the scale surface, counteracting the adhesion forces. Therefore, an increase in the flow velocity may either increase the fouling rate (mass transfer controlled) or decrease it if the interfacial shear has the greater effect (surface integration controlled).

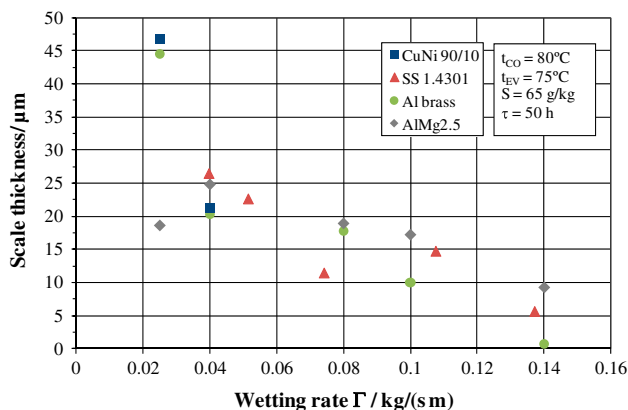


Fig. 11. Effects of the wetting rate on the average scale thickness for different tube materials after a test period of 50 h, $t_{EV} = 75^\circ\text{C}$, $t_{CO} = 80^\circ\text{C}$, $S = 65 \text{ g/kg}$.

Gazit and Hasson [26] studied the mechanism of CaCO_3 scale deposition from an evaporating laminar falling film on a vertical tube. They developed a kinetic model describing scale layer growth assuming that the crystallization surface reaction controls the fouling process. Hasson and Perl [27] extended the previous study and made a more fundamental analysis of transport processes occurring during scale deposition in a laminar falling film system. They concluded that the diffusional effects can be of importance even in thin film flow.

As in vertical tube falling film systems, a falling film on horizontal tubes creates a resistance to heat and mass transfer in the laminar flow regime. Heat and mass transfer decrease with increasing wetting rate and film thickness. Except at very low film Reynolds numbers with the flow being laminar, liquid films develop an interfacial wave structure which increases heat and mass transfer rates above those obtained for smooth liquid film flows. With increasing flow rate and film Reynolds number, the wavy-laminar flow changes to turbulent flow. In their review, Ribatski and Jacobi [28] summarized that in convection-dominated conditions, as the flow rate increases, the heat transfer coefficient decreases first, but increases after a minimum value. This minimum might represent a transition from laminar to turbulent film flow. They pointed out that the heat transfer coefficient was also found to be almost independent of the flow rate and it was found to increase with the flow rate.

Assuming the crystallization fouling process to be diffusion controlled and the resistance to mass transfer to increase with increasing wetting rate and film thickness in the wavy-laminar regime, an increase in wetting rate may reduce the fouling rate, as shown in Fig. 9. A decrease in the mass transfer resistance with increasing wetting rate would rather tend to enhance the fouling rate. But at the same time, an increase in the wetting rate also intensifies the interfacial shear stress on the scale surface, counteracting the adhesion forces. It is known that the adhesion forces are sufficiently high so that shear stress removal effect is absent in the deposition of a scale layer consisting of a pure uncontaminated crystalline substance [10]. However, for mixed salt precipitation, it is believed that shear stress removal may lead to asymptotic fouling behaviour [10].

The wetting rate also influences heat transfer and, thus, the surface temperature which in turn affects crystallization fouling. As described above, some heat transfer models predict an increase in the heat transfer coefficient with the increasing wetting rate (e.g. [20]), others predict a decrease (e.g. [29]) in the

wavy-laminar regime. Thus, the surface temperature may be reduced or increased.

The enhanced scaling tendency at low wetting rates, as shown in Fig. 9, may also be attributed to the variation in the film thickness. The film thickness significantly decreases with the decreasing wetting rate. Hodgson et al. [30] assumed that in the vertical tube falling film evaporators, high local solution concentrations, exceeding the average brine concentration, are formed by fluid elements having either the smallest thickness or residing for a longer period of time in the film.

Furthermore, the co-precipitation of the calcium- and magnesium-containing salts might play an important role. The effect of tube material on the co-precipitating calcium- and magnesium-containing salts in a sea water environment is poorly understood. It is conceivable that some tube materials promote the formation of magnesium-containing scale, for example the magnesium-containing aluminium alloy, which in turn influences the precipitation of calcium carbonate scale.

In previous experiments with CuNi 90/10 tubes [24], a thin Mg-rich scale layer formed on the tube surface even at a low evaporation temperature of 50 °C which promotes the assumption of locally high pH values at the metal–solution interface. A shift in pH to high values in the sea water film due to CO₂ release and, additionally, cathodic reactions resulting in a locally enhanced OH⁻ concentration may promote a high degree of supersaturation of Mg(OH)₂ to drive its rapid precipitation on the tube surface. The quantity of the Mg-rich scale on the CuNi 90/10 tubes did not notably change with increasing test period, ionic strength or in experiments with a calcium-depleted or calcium-free model solution. The present study shows that the magnesium content in the scale does not notably change for CuNi 90/10, Al brass and SS 1.4301 tubes at varying wetting rates. This observation supports the notion that the Mg-rich base layer forms in the early stages and its growth ceases and aragonite crystals start to precipitate once the tube surface is completely covered with the Mg-rich scale layer.

While the calcium content decreases with the increasing wetting rate for all the tube materials and the magnesium content does not notably change for CuNi 90/10, Al brass and SS 1.4301 tubes, the results suggest that the magnesium content on the AlMg2.5 tubes increases with the increasing wetting rate from 0.025 to 0.1 kg/(s m), as shown in Fig. 10. However, at a high wetting rate of 0.14 kg/(s m), the magnesium content in the scale falls to a level which is similar to the one at a low wetting rate of 0.025 kg/(s m). Further work is needed to study co-precipitation of

calcium- and magnesium-containing salts on aluminium alloys.

4. Conclusions

The wetting behaviour of aluminium brass, copper–nickel 90/10, aluminium alloy AlMg2.5 and stainless steel 1.4301 tubes was investigated in a horizontal tube falling film evaporator. In tests with stepwise increasing and decreasing wetting rates, pictures were taken of the film flow over the tubes. The percentages of the wet surface areas on the tube surfaces were evaluated. The wet surface area increases with wetting time at a constant wetting rate. A hysteresis between the wet surface areas occurring at the increasing and decreasing wetting rate was found. The wettability of the different tube materials with deionized water was found to be in the order of Al brass > AlMg2.5 > CuNi 90/10 > SS 1.4301 and with sea water in the order of AlMg2.5 > Al brass > CuNi 90/10 > SS 1.4301 which corresponds to the results of the contact angle measurements. All tube materials show a better wettability with artificial sea water than with deionized water. The results suggest that the physical/chemical effects between metal surface and sea water cause an increase in the wet surface areas with sea water. Furthermore, higher liquid temperatures lead to a better wettability of the tube surfaces caused by a decrease in surface tension and viscosity.

Moreover, the effect of the wetting rate on composition and quantity of mixed salt scale was studied for aluminium brass, copper–nickel 90/10, aluminium alloy AlMg2.5 and stainless steel 1.4301 tubes in the horizontal tube falling film evaporator. The wetting rate was varied in a range between 0.025 and 0.14 kg/(s m), which corresponds to film Reynolds numbers of 56–313 and leads to a wavy-laminar film flow. The tube surfaces were covered with a flaky magnesium-rich base layer and a thick layer of calcium carbonate in the form of aragonite. The mass of calcium in the scale per unit tube surface area increases with the decreasing wetting rate for all the tested tube materials. While the magnesium mass in the scale per unit tube surface area was low on the CuNi 90/10, Al brass and SS 1.4301 tubes and did not notably change with the wetting rate, the magnesium mass was relatively high on the AlMg2.5 tubes, which suggests that the magnesium-containing scale has a higher affinity to aluminium alloys than to copper alloys or stainless steel grades. The average thickness of the scale layer increases with the decreasing wetting rate which corresponds to the increasing calcium carbonate content. The increase in CaCO₃ deposition with the decreasing wetting rate was discussed in

the light of film thickness, flow velocity, mass transport and co-precipitation of calcium- and magnesium-containing salts in the wavy-laminar falling film.

Symbols

d_0	outside diameter of tubes, m
L	length of tubes, m
\dot{m}	mass flow rate, kg/s
R_a	surface roughness, μm
Re_F	film Reynolds number, -
S	salinity, g/kg
s	tube pitch, m
t_{CO}	condensation temperature, $^{\circ}\text{C}$
t_{EV}	evaporation temperature, $^{\circ}\text{C}$
\bar{u}	average flow velocity, m/s

Greek symbols

Γ	wetting rate, kg/(s m)
Γ_{crit}	critical wetting rate, kg/(s m)
γ_{lv}	liquid–vapour interfacial tension, mN/m
γ_{sl}	solid–liquid interfacial tension, mN/m
γ_{sv}	solid–vapour interfacial tension, mN/m
δ	film thickness, m
η	dynamic viscosity, Pa s
θ	contact angle, $^{\circ}$
ρ	density, kg/m ³
τ	test period, h

References

- [1] H. Müller-Steinhagen, Verminderung der Ablagerungsbildung in Wärmeübertragern (Mitigation of fouling in heat exchangers), in: VDI-Gesellschaft (Ed.), VDI-Wärmeatlas (VDI Heat Atlas), Springer-Verlag, Berlin Heidelberg, 2013, pp. 91–121.
- [2] J.W. Vermey, Taweelah-A1 makes breakthrough in large-scale MED plants, *Int. Desalin. Water Reuse Q.* 12(4) (2003) 9–13.
- [3] X. Zhao, X.D. Chen, A critical review of basic crystallography to salt crystallization fouling in heat exchangers, *Proceedings of International Conference on Heat Exchanger Fouling and Cleaning*, Crete Island, Greece, 2011.
- [4] T. Geddert, I. Bialuch, W. Augustin, S. Scholl, Extending the induction period of crystallization fouling through surface coating, *Heat Transfer Eng.* 30 (2009) 868–875.
- [5] Y. Yuan, T.R. Lee, Contact angle and wetting properties, in: G. Bracco, B. Holst (Eds.), *Surface Science Techniques*. Springer-Verlag, Berlin Heidelberg, 2013, pp. 3–34.
- [6] T. Young, An essay on the cohesion of fluids, *Philos. Trans. R. Soc. Lond.* 95 (1805) 65–87.
- [7] V. Baujat, T. Bukato, Research and development towards the increase of MED units capacity, *Proceedings of IDA World Congress on Desalination and Water Reuse*, Bahamas, 2003.
- [8] R. Greffrath, Effect of scaling on design and operation of thermal seawater desalination plants, in: H. Glade, J. Ulrich (Eds.), *Scaling in Seawater Desalination: Is Molecular Modeling the Tool to Overcome the Problem?* Shaker Verlag, Aachen, 2001, pp. 15–32.
- [9] R. Greffrath, MED, MED-TVC Design II. Process design optimisation, *Proceedings of DME Workshop “Thermal Desalination of Saline Waters”*, Duisburg, 2012.
- [10] D. Hasson, Scale formation and prevention, in: H. Glade, J. Ulrich (Eds.), *Scaling in Seawater Desalination: Is Molecular Modeling the Tool to Overcome the Problem?* Shaker Verlag, Aachen, 2001, pp. 49–68.
- [11] T.M. Pääkkönen, M. Riihimäki, C.J. Simonson, E. Muurinen, R.L. Keiski, Crystallization fouling of CaCO₃—Analysis of experimental thermal resistance and its uncertainty, *Int. J. Heat Mass Transfer* 55 (2012) 6927–6937.
- [12] A. Helalizadeh, H. Müller-Steinhagen, M. Jamialahmadi, Mixed salt crystallization fouling, *Chem. Eng. Process.* 39 (2000) 29–43.
- [13] D. Hasson, M. Avriel, W. Resnick, T. Rozenman, S. Windreich, Mechanism of calcium carbonate scale deposition on heat-transfer surfaces, *Ind. Eng. Chem. Fund.* 7(1) (1968) 59–65.
- [14] W. Augustin, M. Bohnet, Influence of the ratio of free hydrogen ions on crystallization fouling, *Chem. Eng. Process.* 34 (1995) 79–85.
- [15] D.R. Kester, I.W. Duedall, D.N. Connors, R.M. Pytkowicz, Preparation of artificial seawater, *Limnol. Oceanogr.* 12 (1967) 176–179.
- [16] F.J. Millero, *Chemical Oceanography*, fourth ed., CRC Press, Boca Raton, FL, 2013.
- [17] M. Förster, M. Bohnet, Modification of molecular interactions at the interface crystal/heat transfer surface to minimize heat exchanger fouling, *Int. J. Thermal Sci.* 39 (2000) 697–708.
- [18] E. Rio, L. Limat, Wetting hysteresis of a dry patch left inside a flowing film, *Phys. Fluids* 18 (2006) 032102.
- [19] J. Gebel, Zum Einsatz von Horizontalrohrverdampfern in Mehrfacheffektanlagen zur Eindampfung wässriger Lösungen (On the use of horizontal tube falling film evaporators in multiple-effect distillers for the evaporation of aqueous solutions), PhD Thesis, Aachen, 1990.
- [20] Y. Fujita, M. Tsutsui, Experimental investigation of falling film evaporation on horizontal tubes, *Heat Transfer Jpn. Res.* 27(8) (1998) 609–618.
- [21] D. Moalem, S. Sideman, Theoretical analysis of a horizontal condenser–evaporator tube, *Int. J. Heat Mass Transfer* 19 (1976) 259–270.
- [22] P.L. Kapitza (Ed.), *Collected papers of P.L. Kapitza*, Vol. 2, Pergamon Press, Oxford, 1965, pp. 662–709.
- [23] W. Wilke, Wärmeübergang an Rieselfilme (Heat transfer to falling films), VDI-Forschungsheft Nr. 490, VDI Verlag, Düsseldorf, 1962.
- [24] H. Glade, K. Krömer, S. Will, K. Loisel, S. Nied, J. Detering, A. Kempter, Scale formation and mitigation of mixed salts in horizontal tube falling film evaporators for seawater desalination, *Proceedings of International Conference on Heat Exchanger Fouling and Cleaning*, Budapest, 2013.
- [25] H. Glade, K. Krömer, A. Stärk, K. Loisel, K. Odiod, S. Nied, M. Essig, Effects of tube material on scale formation and control in multiple-effect distillers,

- Proceedings of IDA World Congress on Desalination and Water Reuse, Tianjin, 2013.
- [26] E. Gazit, D. Hasson, Scale deposition from an evaporating falling film, *Desalination* 17 (1975) 339–351.
- [27] D. Hasson, I. Perl, Scale deposition in a laminar falling-film system, *Desalination* 37 (1981) 279–292.
- [28] G. Ribatski, A.M. Jacobi, Falling-film evaporation on horizontal tubes—A critical review, *Int. J. Refrig.* 28 (2005) 635–653.
- [29] B. Arzt, Meerwasserentsalzung durch Mehrfach-Effekt-Stack Horizontalrohrverdampfung—Verfahrensentwicklung und Designstudien (Sea water desalination by multiple-effect stack horizontal tube falling film evaporation-process development and design studies), PhD Thesis, Aachen, 1984.
- [30] T.D. Hodgson, M.N. Elliot, T.W.J. Jordan, Calcium sulphate scaling in falling film evaporators, *Desalination* 14 (1974) 77–91.